中國機械工程學刊第四十一卷第三期第 381~389 頁(民國一百零九年)
Journal of the Chinese Society of Mechanical Engineers, Vol.41, No.3, pp 381~389(2020)

Optimal Design of a Hybrid Cable Driven Parallel Robot for Desired Trajectory and Wrench Box

Chawalit Khanakornsuksan* and Theeraphong Wongratanaphisan**

Keywords: Hybrid Cable Driven Robot, PSO algorithm, Dimensional Synthesis, Optimal Design

ABSTRACT

A hybrid cable-driven planar parallel robot (HCDPPR) is a parallel mechanism which exploits the high-force capacity of cables in combination with rigid links. In this study, method for optimal design synthesis of the HCDPPR is presented. The HCDPPR considered consists of a serial link chain, one linear actuator and two actuating cables. The linear actuator together with the two cables produce three-degree-of-freedom motion for a mobile platform (MP) in a vertical plane. These cables help to reduce system inertia and increase workspace compared to all-rigid-linkage system. The rigid links help to avoid redundant actuating requirement and potential cable tangling problem that may occur in an all-cable system. The location of cable attachments and size of connecting rod are the function of cable tension and MP motion which affect to the capability of motor. In this study, an optimal design method, based on particle swarm optimization (PSO) is proposed to minimize cable tensions for a range of given wrenches applied on the MP. The constraints are the path that the MP must follow over a range of MP's orientation and the cables are always in tension. Optimized parameters include the position of cable attachment on the base and rigid link, the length of the rigid link and mass of MP. In addition, the wrench box is included in the design algorithm to include the uncertainty wrench over operation. The optimal design method will be suitable for many proposes. Examples that demonstrate how optimized algorithm works are given. The proposed structure of the robot has potential for use an automatic gait machine as cables can provide large range of motion and high force requirement.

Paper Received March, 2019. Revised September, 2019, Accepted September, 2019, Author for Correspondence: Theeraphong Wongratanaphisan

[*]*Ph. D student, Graduate Program, Department of Mechanical Engineering, Chiang Mai University, Chiang Mai, Thailand, 50200*

[**]*Associate Professor, Department of Mechanical Engineering, Chiang Mai University, Chiang Mai, Thailand, 50200*

INTRODUCTION

Cable Driven Planar Parallel Robot (CDPPR) is a special class of Parallel Kinematic Manipulator (PKM) whose actuated limbs are cables instead of rigid-link actuators. All cables are attached to a mobile platform, referred to as the "end-effector". The other end of cables is wound on actuating drums which is fixed to ground. A mobile platform (MP) can be programmed to move along pre-defined trajectories / poses (position and orientation) in task space by varying the cable's length but this has to be carried out while all cables are taut (Roberts, Graham et al. 1997). The motors located at the base are fixed. The cables replace some rigid-link components which then help to reduce system's inertia. The benefits are high payload-to-weight ratios, large workspace, transportability and reconfigurability. A number of researchers have applied cable robots in many tasks such as pick-and-place, measurement, haptics, high-speed manipulator, simulator and rehabilitation.

The shape and size of the workspace depends on geometric arrangement of the actuated reels on the base and the attachment points of the cable on MP. Several researchers have proposed methods to dimensionally synthesize the CDPM by discretization-based method (Hay and Snyman 2005). Another approach is to synthesize the CDPM from a given prescribed workspace. Hay and Snyman (2005) maximized the area of the dexterous workspace by relocating cable attachment points, while cable tension is constrained to lie within a given tension set. Azizian and Cardou (2013) proposed methodologies for determining the optimum geometry by maximizing the shape and size of the Wrench Closure Workspace Convex prescribed pose box. To include the external wrench, the available wrench set can be represented

mathematically by a zonotope, a special class of convex polytope (see Bouchard et al. (2010) and Azizian et al. (2012)). Bosscher et al. (2006) have determined the maximum size of the task which covered by the zonotope of desired architecture. However, their work still lacks consideration on the dimensional synthesis of a Wrench Feasible Workspace (WFW). The dimensional synthesis with WFW will provide the optimized mechanism which can work on the desired trajectory while external wrenches applying on MP along the path.

Unlike rigid links, cables can only provide unidirectional force (pulling force). There must be at least one more cable than the number of degrees of freedom (DOF) to avoid slack in cables (Pham, Yeo et al. 2006, Gouttefarde 2008). As planar CDPPRs have great potential for use in many applications, this study tries to reduce the number of cables with the new design that uses two actuating cables in combination with a linear actuating slider connected to MP via a connecting rod. There are some but not many studies that considered integrating rigid links into cable driven systems, for example, cable driven robot finger design. However, those systems the arrangement of the cable are not parallel in nature. In this study, we propose to include rigid into cable driven parallel robot structure.

The proposed structure is a "Hybrid Cable-Driven Planar Parallel Robot" (HCDPPR). The linear actuator supplies force to produce motion in a horizontal direction. One cable is attached to the MP and another attached to the rigid link. This machine can generate 3 DOF motion of MP: (x- and y- position and orientation in a vertical plane). The robot design aims to produce a smooth motion for a pre-defined pose. To optimize the performance of the HCDPPR, locations of actuators and attachment point on MP need to be properly determined for given task space. For robustness, in the synthesis, bounded uncertainties will be added to the external wrench applied on MP. For planar mechanism, the external wrench is, hence, defined as a three-dimensional box shape. The proposed methodology is applied to a HCDPPR to obtain optimized mechanism which can move along pre-defined pose and withstand the external wrenches with some uncertainties while ensuring that all the cables are always in tension.

The remainder of this paper is organized as follows. First, concept design of a HCDPPR is described in Section 2. Section 3 provides the conditions requirements and analysis involved in the optimization algorithm. Section 4 demonstrates the method with example trajectory and external wrench box. Conclusions are given in Section 5.

HYBRID CABLE DRIVEN PLANAR PARALLEL ROBOT

Description

Figure 1 shows a full cable-driven planar robot. To generate 3-DOF motion on a plane, it is required that at least 4 actuating cables are installed. This over-actuating requirement is to help cope with requirement that all cables have positive tension: the number of actuators needs to be higher than the degree of freedom. This deficit leads to the notion of replacing two cables with a rigid member that can provide both compression and tension forces — hence reducing actuating members to only three. In this study we are interested in a hybrid cable-driven planar parallel robot (HCDPPR) as a candidate for automated gait machine.

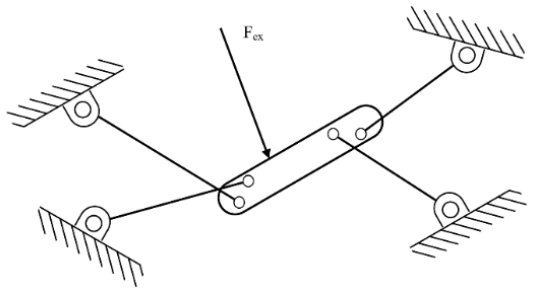

Fig. 1. A general fully CDPPR configuration in a vertical plane

Figure 2, shows the proposed structure of the mechanism. It is a 3- DOF mechanism operating in a vertical plane. Frame{1}, origin at O_1, is attached to the frame of linear actuator (labeled 2). This actuator can supply both pushing or pulling force which is then transmitted to MP via a rigid rod (labeled 3). Frame{2}, origin at O_2, is attached to the MP. The linear actuator, mass m_p, moves on a horizontal line y_1. The connecting rod, mass m_b, moment of inertia I_b and length l_b, is connected between the piston and the MP at $O_1(x_1, y_1)$ and $O_2(x, y)$, respectively. Two cables (labeled 5 and 6) are attached to ground at ${}^{pf}A_2(a_{2x}.a_{2y})$ and ${}^{pf}A_3(a_{3x}.a_{3y})$, respectively. The other ends of cable are located at $X_2(x_2, y_2)$ and $X_3(x_3, y_3)$. The configuration is designed for the two cables to carry the downward external forces. The rigid link will help to move MP along the desired trajectory with prescribed orientation while the cables are always in tension (zero or negative tension is not allowed).

Kinematic Analysis

Let $q = [x_1, \beta, \gamma]$ be a vector of generalized coordinates. Given the desired trajectory (x, y) of MP, the angle of connecting rod β can be calculated by

$$\beta = \arctan\left(\frac{\sin\beta}{\cos\beta}\right) \quad (1)$$

where, $\sin\beta = \frac{F_y - y_1}{l_b}$ and $\cos\beta = \pm\sqrt{1-\sin^2\beta}$. Therefore, From the inertial frame OXY, the position of linear actuator is determined by

$$x_1 = x - l_b\cos\beta \quad (2)$$

The position vector of the moving piston is determined from the origin of Frame{1}. The position vector of piston is represented as vector $[x_1, y_1]$. The position vector of cable attached point are $\boldsymbol{X_2A_2}$ and $\boldsymbol{X_3A_3}$:

$$\boldsymbol{X_2A_2} = \begin{bmatrix} x_1 + a_{2x}\cos\beta \\ y_1 + a_{2x}sin\beta \end{bmatrix} \quad (3)$$

$$\boldsymbol{X_3A_3} = \begin{bmatrix} x_1 + l_b\cos\beta + a_{2x}\cos\beta \\ y_1 + l_b\sin\beta + a_{2x}sin\beta \end{bmatrix} \quad (4)$$

The lengths of the cables l_2 and l_3 which are the magnitude of vector $\boldsymbol{X_2A_2}$ and $\boldsymbol{X_3A_3}$ are used to determine the Jacobian matrix. For a prescribed path, $q, \dot{q}, \ddot{q}$ can be determined through inverse kinematic analysis in Eqs. (1) to (4). The velocity of the moving guide is $\boldsymbol{v_1} = \frac{d\boldsymbol{OO_1}}{dt}$ and the velocities of the cable attached point on MP are $\boldsymbol{v_b} = \frac{d\boldsymbol{X_2A_2}}{dt}$ and $\boldsymbol{v_{pf}} = \frac{d\boldsymbol{X_3A_3}}{dt}$, respectively.

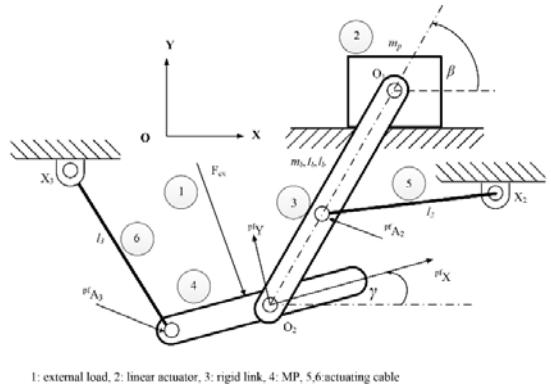

1: external load, 2: linear actuator, 3: rigid link, 4: MP, 5,6:actuating cable

Fig. 2. The configuration of the hybrid cable driven robot

Dynamics Analysis

The cable masses are assumed to be negligible and the attachment points on the MP are assumed to be representable by a spherical joint. The equations of motion of the system can be obtained by the Lagrange's method. Let $\boldsymbol{Q}$ be generalized force vector obtained from mapping the applied actuator force T_2 and T_3, and linear actuator F_{x1}, through the Jacobian matrix $\boldsymbol{J}$ to balance the external force vector $\boldsymbol{F_{ex}}$. Then the dynamic of the mechanism can be written in the form:

$$\boldsymbol{M}\ddot{q} + \boldsymbol{N}(\dot{q}, q) + \boldsymbol{G} = \boldsymbol{Q} + \boldsymbol{Q_{ex}} \quad (5)$$

$\boldsymbol{M}$ is the symmetric positive-definite inertia matrix. $\boldsymbol{N}$ is an n_d - dimensional vector of centrifugal and Coriolis forces. $\boldsymbol{G}$ represents a vector of gravitational force (the components of these matrices are shown in the Appendix). There are 3 external forces associated with generalized coordinates x_1, β and γ:

$$Q_{ex,i} = \sum_{j=1}^{3} \boldsymbol{W_{ex}} \cdot \frac{\partial \boldsymbol{OO_2}}{\partial q_i} \quad (6)$$

where

$\boldsymbol{W_{ex}} = [RF_x \quad RF_y \quad RM_z]^T$,

$\boldsymbol{OO_2} = [OO_{2x} \quad OO_{2y} \quad OO_{2z}]^T$.

There are also 3 generalized forces associated with generalized coordinates x_1, β and γ:

$$Q_i = \sum_{j=1}^{3} \boldsymbol{T_j} \cdot \frac{\partial \boldsymbol{L_j}}{\partial q_i} \quad (7)$$

Where

$\boldsymbol{T} = [\boldsymbol{F_{x1}} \quad \boldsymbol{T_2} \quad \boldsymbol{T_3}]$, $\boldsymbol{L} = [\boldsymbol{OO_1} \quad \boldsymbol{X_2A_2} \quad \boldsymbol{X_3A_3}]$ and $\boldsymbol{Q} = [Q_{x1} \quad Q_\beta \quad Q_\gamma]^T$.

These generalized forces are associated with matrix $\boldsymbol{J}$ and the actuators force vector $\boldsymbol{T}$:

$$\boldsymbol{Q} = \boldsymbol{J} \cdot \boldsymbol{T} \quad (8)$$

where $J_{ij} = \boldsymbol{u_j} \cdot \frac{\partial \boldsymbol{L_j}}{\partial q_i}$ and $\boldsymbol{u_j}'s$ are a unit vector of actuator j. For a given motion, i.e., known $q, \dot{q}, \ddot{q}$, the equation of motion Eq. (5) and generalized force Eqs. (6) to (8) are used to determine the actuator forces:

$$\boldsymbol{T} = \boldsymbol{J}^{-1}(\boldsymbol{M}\ddot{q} + \boldsymbol{N}(\dot{q}, q) + \boldsymbol{G} - \boldsymbol{Q_{ex}}) \quad (9)$$

OPTIMAL DESIGN AND ALGORITHM

To move the MP along prescribed path while also withstanding the external wrenches, the actuating cables and the linear actuator must be able to supply the forces accordingly. The level of the actuating force required to perform such tasks will depend on the location of the cable attachment points to MP and ground. In practice, we would like the level of these actuating forces to be as small as possible which means smaller actuators are required. Therefore, the optimal design problem here is defined in terms of reducing actuating forces under applied external wrench during the prescribed motion. The external wrenches are defined in terms of the ranges of external force and moments that apply on the MP and these ranges will be represented by a polygonal wrench box.

Given the non-linear terms in the dynamic equation, Eq. 9, the design optimization of the HCDPPR is a non-linear problem which contains many locally optimal solutions. In general, one prefers to obtain the global optimal solution when possible. Bruckmann, Mikelsons et al. (2009) introduced many kinds of the optimization problems and solutions. They suggested combine multiple optimizer techniques to obtain better optimized results. Particle Swarm Optimization (PSO) is one of the techniques which combines the simple optimization algorithm with the social update rule (Kulkarni, Patekar et al. 2015). This optimizer is suitable for this global optimization problem and will be used in this study.

Particle Swarm Optimization (PSO) Algorithm

For PSO, an initial population is the set of solutions which are evolved/updated to explore the search space by sharing communication (Shen, Zhu et al. 2009, Bryson, Jin et al. 2016). To apply this

technique, the optimization system is set as shown in Fig. 3.

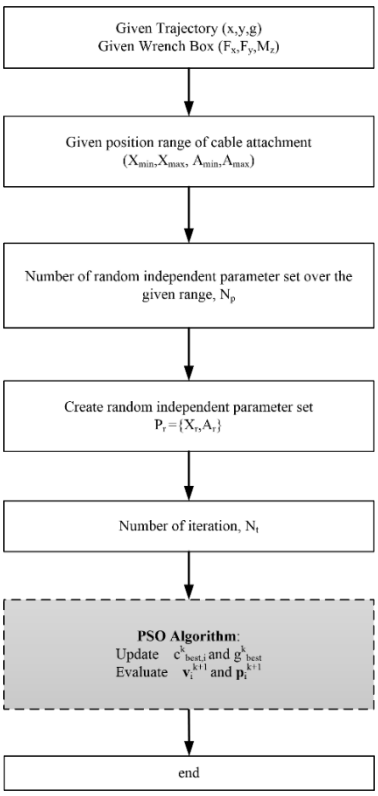

Fig. 3. PSO algorithm concept design for HCDPPR

The optimized parameters are the position of cable attachment, the length of the connecting rod, and the mass of the MP. For problem considered here, there are a total of 10 optimized parameters (N_v) which are contained in vector $\boldsymbol{p}$.

The searching space of each parameters are independent but bounded by $[\boldsymbol{LB}\ \boldsymbol{UB}]$ where $\boldsymbol{LB}$ and $\boldsymbol{UB}$ are the vectors of lower bound and upper bound values of these parameters (the components of these vectors are shown in the Appendix). The PSO searches for solutions through iteration loops. Define the number of iterations as N_k and the number of optimized vectors $\boldsymbol{p}$ as N_p. At iteration k, the configuration vector is formed as $\boldsymbol{P}^k = \left[\boldsymbol{p}_1^k, \dots, \boldsymbol{p}_{n_p}^k, \dots, \boldsymbol{p}_{N_p}^k\right]_{N_v \times N_p}$. It consists of N_p configuration vectors in searching space and each vector has N_v elements. The PSO is initialized by a random group $\boldsymbol{P}^1$. Define matrix $\boldsymbol{P}^1 = \left[\boldsymbol{p}_1^1, \dots, \boldsymbol{p}_{n_p}^1, \dots, \boldsymbol{p}_{N_p}^1\right]_{N_v \times N_p}$ which contains initial randomly searching solution vectors. Each component in solution vector $\boldsymbol{P}^k$ is updated according to the two best values: $\boldsymbol{C}_{best}^{k-1}$ and $\boldsymbol{g}_{best}^{k-1}$. $\boldsymbol{C}_{best}^{k-1}$ is a vector of a local best configuration of each $\boldsymbol{p}_n^{k-1}$. $\boldsymbol{g}_{best}^{k-1}$ is a vector of global best configuration. Figure 4 show the concept of the update algorithm based on PSO which can be explained as follows.

Here,

$$\boldsymbol{c}_{best,n_p}^k = \begin{cases} \boldsymbol{c}_{best,n_p}^{k-1} & f\left(\boldsymbol{c}_{best,n_p}^k\right) > f\left(\boldsymbol{c}_{best,n_p}^{k-1}\right) \\ \boldsymbol{c}_{best,n_p}^k & f\left(\boldsymbol{c}_{best,n_p}^{k-1}\right) > f\left(\boldsymbol{c}_{best,n_p}^k\right) \end{cases} \tag{10}$$

$\boldsymbol{c}_{best}^k$ is the solution vector of $\boldsymbol{P}^k$ which is $\min\left(f\left(\boldsymbol{c}_{bset}^k\right)\right) < \min\left(f\left(\boldsymbol{c}_{bset,n_p}^k\right)\right)$ for k^{th} iteration and

$$\boldsymbol{g}_{best}^k = \begin{cases} g_{best}^{k-1} & f\left(c_{best}^k\right) > f\left(g_{best}^{k-1}\right) \\ c_{best}^k & f\left(g_{best}^{k-1}\right) > f\left(c_{best}^k\right) \end{cases} \tag{11}$$

At current k^{th} iteration, $\boldsymbol{P}_{n_p}^{k+1}$ is individually updated according to the values $\boldsymbol{C}_{best}^k$ and $\boldsymbol{g}_{best}^{k-1}$:

$$\boldsymbol{v}_{n_p}^{k+1} = w \cdot \boldsymbol{v}_{n_p}^k + c_1 \cdot r_1 \cdot \left(\boldsymbol{c}_{best,n_p}^k - \boldsymbol{P}_{n_p}^k\right) + c_2 \cdot r_2 \cdot \left(\boldsymbol{g}_{best}^k - \boldsymbol{P}_{n_p}^k\right) \tag{12}$$

$$\boldsymbol{p}_{n_p}^{k+1} = \boldsymbol{p}_{n_p}^k + \boldsymbol{v}_{n_p}^{k+1} \tag{13}$$

where $\boldsymbol{P}_{n_p}^{k+1}$ and $\boldsymbol{v}_{n_p}^{k+1}$ are the updated solution and trended toward $\boldsymbol{g}_{best}^k$, respectively. $\boldsymbol{P}_{n_p}^k$ is the current solution. $\boldsymbol{v}_{n_p}^k$ is the magnitude and direction of change trended toward $\boldsymbol{g}_{best}^k$. w is the weighting of inertia (Marini, Walczak et al. 2015). The suitable value of w can be determined from $\frac{1}{2}(c_1 + c_2) - 1 < w < 1$ for $0 < (c_1 + c_2) < 4$, (Bryson, Jin et al. 2016). c_1 and c_2, called the learning factor, are positive acceleration constant trends toward the local and global optimum values, respectively. r_1 and r_2 are then random numbers uniformly distributed in a range [0,1].

After k^{th} iteration, the algorithm shows the best solution which is recorded in vector g_{best}^k. The algorithm stops the iteration loop if the change in objective value is small enough compared to the value in the previous iteration.

OPTIMIZATION RESULTS AND DISCUSSION

Prescribed Trajectory and Wrench Box

Let the desired position (x, y) of the MP be defined as a circle of radius 0.5 m shown in Fig. 5(a). In addition, along the path shown the MP must be able to rotate with angle γ in the range of $\left[-\frac{\pi}{4}\ \frac{\pi}{4}\right]$. Along the prescribed motion above, the MP must also be able to resist the external wrench box. This box can be defined as a 3-dimensional polygonal shape in wrench space, $F_x - F_y - M_z$. The range of each dimension can be viewed as uncertainty with the lower and upper limits that may be applied to the MP. Here these external wrenches are considered to be contained in polygonal box ranging between $[-10\ 10]$ for each dimension as shown in Fig. 5(b).

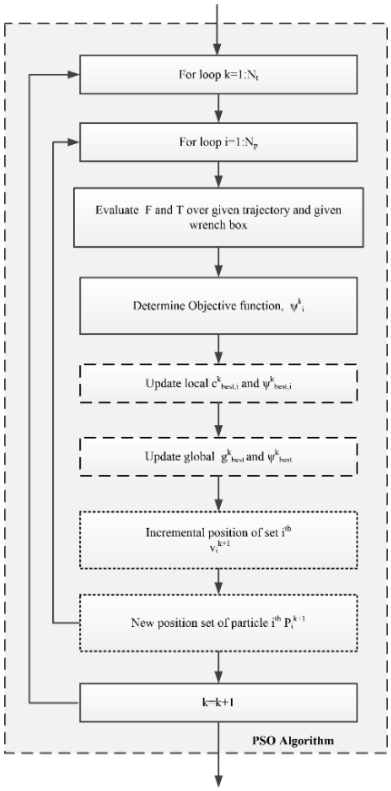

Fig. 4. PSO algorithm concept for N_p particles and N_k iterations

To achieve the objective, task completion must be verified with constraint(s) which ensure that the desired pose defined in the task space, TW which is the subset of the system workspace, SW . The workspace SW depends on the configuration. Operating wrench boxes, W_{ex} must be within the wrench system workspace, WSW . W_{ex} can be any shape in wrench dimension, which in this paper has been defined as parallelepiped box. W_{ex} may be defined as exact wrench profile without uncertainty but this is prone to failure as uncertainties if exist can cost the cable to sag. Defining the wrench profile to be within the wrench box increases the effectiveness of the system to work with uncertainty. While all conditions are satisfied, all cable tensions will always be positive. These can be formulated as constrained optimization problem which is defined as follows:

Given: the trajectory and the external wrenches to be applied on MP

find: the locations of cable attachment on MP and ground, length of rigid bar and length of MP and mass of MP (all parameters are contained in vector $\boldsymbol{P}$).

such that: summation of the peaks of all actuator forces during the motion are minimized.

with constraints:

1) tension forces in the cables are always positive and stay within the bound values $[T_{min} \quad T_{max}]$.
2) the installed cable locations and other optimal parameters in $\boldsymbol{P}$ are within the bounded values [$\boldsymbol{LB}$ $\boldsymbol{UB}$].

The optimization problem defined above can be represented mathematically as:

$$\varphi = \min \sum_{i=1}^{N_i} \|T_i(\boldsymbol{P})\| \tag{14}$$

subject to

$TW \subseteq \text{SW}$, $W_{ex} \subseteq \text{WSW}$,

$T_1 \in [F_{1,min} \quad F_{1,max}]$, $T_2, T_3 \in [T_{min} \quad T_{max}]$,

$T_{min} > 0$, $\boldsymbol{T}(\boldsymbol{P}) = \boldsymbol{J}^{-1}(\boldsymbol{M}\ddot{q} + \boldsymbol{N}(\dot{q}, q) + \boldsymbol{G} - \boldsymbol{W_{ex}}$,

$\boldsymbol{P} \leq \boldsymbol{UB}$ and $\boldsymbol{P} \geq \boldsymbol{LB}$ (15)

where $\boldsymbol{T}(\boldsymbol{P})$ is the actuator forces at pose (x_j, y_j, γ_j) which is determined from the equations of motion, Eq. (9), with the optimized parameters $\boldsymbol{P}$.

The solution is only feasible if all the constraints are satisfied. Note that, the optimized actuator force must satisfy the equations of motion and remain within some specified upper and lower bounds. In general, the amount of tension required to avoid the slackness is the lower bounded value, while the upper limit corresponds to the torque capability of the motors and the failure stress of the cables. The actuator limits are bounded by $T_i = [T_{i,min} \quad T_{i,max}]$.

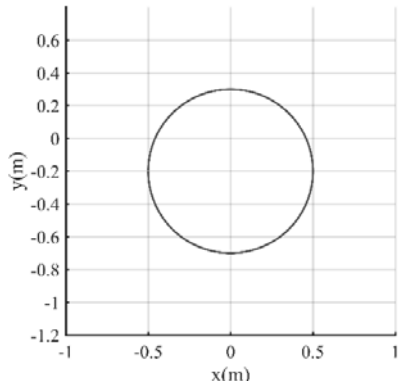

(a) Pose profile

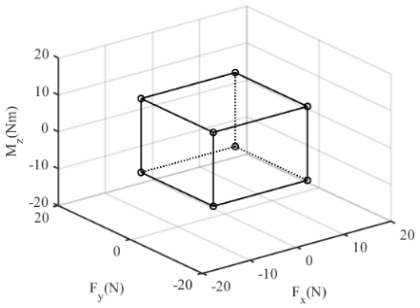

(b) force profile

Fig. 5. Pose and force profile in the desired trajectory

Optimization Results

Table 1 presents the list of parameters used to demonstrate the result of the design. The MP moves along the desired trajectory which circle path shown in Fig. 5(a) with the constant path velocity of 0.94 m/s in

counterclockwise direction. At each point, the orientation is also assumed to be able to change within (-45,45) degrees. The path line was divided into 334 discrete points. All the optimization algorithm will be applied at these points. The connecting rod has mass of 2 kilograms. The linear actuator moves along the horizontal line at level y_o with travel length Δx_1. The motion of linear actuator transforms to MP by a connecting rod. Applying PSO to the optimization problem in Eq. (14) for the design variable parameters in Eq. (15), a task-optimized design of HCDPPR is obtained by population size, n_p, of 10,000 (10,000 particles). The external wrench boxes are shaped in $[-10\ 10]$N, $[-10\ 10]$N and $[-10\ 10]$Nm for F_x, F_y, and M_z, respectively. Table 2 shows the global optimized parameter for each iteration and the objective trend is shown in Fig. 6.

Table 1. The boundary of the optimal parameter

parameter	X_2	Y_2	X_3	Y_3	A_{2xf}	A_{3xf}	l_b	y_0	m_{pf}	b_f
LB	-2	-2	-2	-2	-0.5	-0.5	-0.5	-5	0.1	-0.5
UB	2	2	2	2	3	0.5	3	5	10	0.5
unit	m	m	m	m	m	m	m	m	kg	m

Table 2. The global solution vector of design parameter of the 1st to 12th iteration, ($\boldsymbol{P}^1$ to $\boldsymbol{P}^{12}$)

$iteration$	1	2	3	4	5	6	7	8	9	10	11	12
X_2(m)	1.10	1.12	1.92	2	2	2	1.99	2	2	2.00	2.00	2
Y_2(m)	-1.97	-1.81	-2	-2	-2	-2	-2	-2	-2	-2	-2	-2
X_3(m)	-0.05	-0.22	-0.50	-0.42	-0.42	-0.60	-0.58	-0.53	-0.54	-0.55	-0.55	-0.55
Y_3(m)	1.63	1.66	2	2	2	2	2	2	2	2	2	2
A_{2xf}(m)	0.98	1.15	1.96	2.73	2.73	3	3	3	3	3	3	3
A_{3xf}(m)	0.09	0.11	0.22	0.23	0.23	0.24	0.23	0.23	0.23	0.23	0.23	0.23
l_b (m)	2.9	2.30	2.77	3	3	3	3	3	3	3	3	3
y_0(m)	0.85	0.60	0.94	0.80	0.80	1.57	1.49	1.21	1.24	1.25	1.25	1.25
m_{pf}(kg)	8.71	8.74	10	10	10	10	10	10	10	10	10	10
b_f(m)	0.41	0.38	0.5	0.5	0.5	0.5	0.5	0.5	0.5	0.5	0.5	0.5

Table 3. The global solution vector of design parameter at kth iteration, ($\boldsymbol{P}^k$)

$iteration$	1	2	3	4	5	6	7	8	9	10	11	12
φ (10^3N)	15.40	10.25	5.496	4.954	4.954	4.774	4.757	4.747	4.743	4.741	4.741	4.741
Δx_1(m)	1.07	1.04	1.06	1.04	1.04	1.18	1.16	1.10	1.10	1.10	1.10	1.10

The results obtained from 1st to 12th iteration are shown in Table 2. The algorithm stopped at 12th iteration as the change of objective value is within 5% of the value in previous iteration. Table 3 shows Δx_1 which is total stroke of linear actuator required for the tasks.

Discussion

The optimization algorithm started with a seat of 10,000 random sets. Through iteration the objective value improved by the updated rule in the PSO algorithm. According to Fig. 6, the objective value converts to 4.741 kN in 4 iterations. Satisfied tensions are shown in Fig.

7(a), (b) and (c) for first, sixth, and twelfth iteration, respectively. The solutions obtained in various steps are shown in Fig.8 and corresponding operating tensions are shown in Fig. 7. The particles solution parameters searched a solution which satisfied all the constraints. Through each iteration, all sets of configuration vectors tried to improve the objective values from the previous step. The configuration shown in Fig. 8(b) is the solution after sixth iteration and its operating tension was shown in Fig. 7(b). Their objective value was reduced from the previous iteration. The sharing social communication featured in the PSO algorithm showed minimal objective to other configuration sets. This affects the new direction of searching of other configuration sets. This technique improves the convergence rate of algorithm, shown in Fig. 6. It is noticed that through iterations, resulted configurations tend to be larger than those from the previous steps. Finally, at the twelfth iteration shown in Fig. 8(c), the optimization process ended as the changes of the objective values is within the set point of 5% of the previous step. The cable attachment at the base satisfies the desired boundary. Note that the upper value of the required actuator forces will depends on the defined boundary of the cable attached location. Increasing this boundary can help reduce the required force capacity of the actuators. However, posting no limit and this boundary will affect the overall footprint of the robot and can be unpractical. This trade-off will need to be considered in the early state of design.

It should be noted that the selection of connecting rod configuration (rod-front and rod-back) will result in a different solution set which may or may not provide better solutions for a given task.

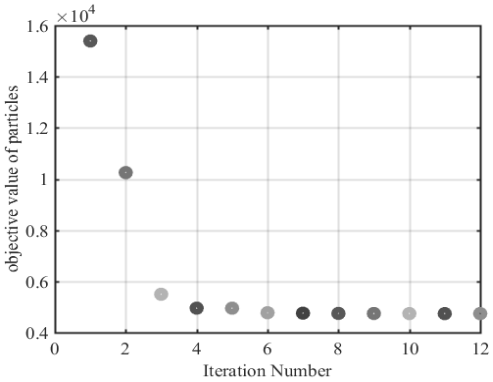

Fig. 6. The convergence of objective values

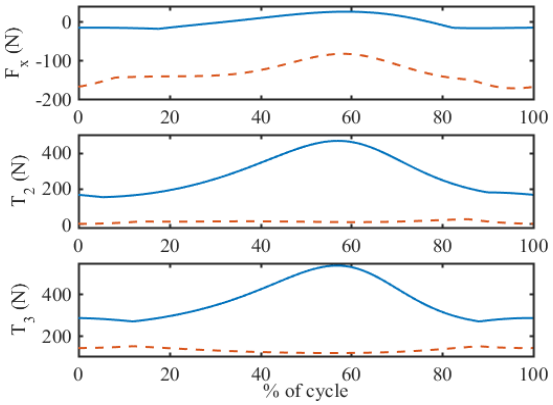

(a) 1st iteration

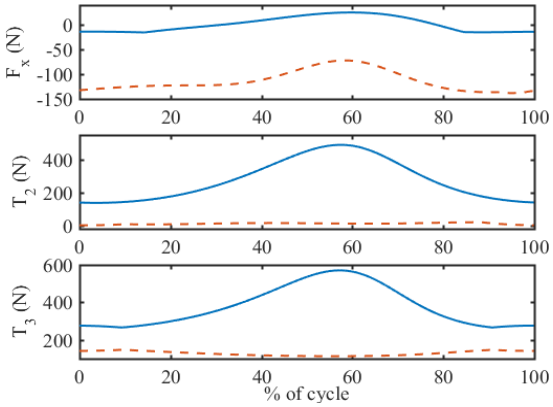

(b) 6th iteration

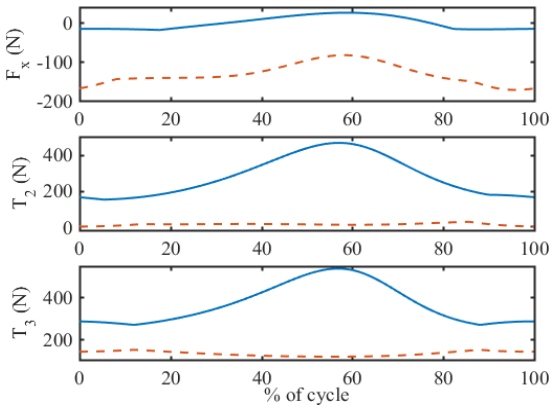

(c) 12th iteration

Fig. 7. The tensions required at sample iteration the solid lines are the maximum boundary and the dot lines are lower bound of each actuator force requirement.

CONCLUSION

In this study, a hybrid cable driven planar parallel robot (HCDPPR) was introduced. This mechanism can generate 3-DOFs motion of MP (x- and y- positions and γ - orientation in a vertical plane). The proposed mechanism was designed with two cables and one rigid link in order to maintain the number of degrees of actuation equal to the number of degrees of freedom. The cables were designed to take only tension force, while the rigid link can take both tension and compression forces. A method was proposed to search the optimal locations of the cable attachment points rigid links and ground while keeping the cable tensions minimized. The mass of MP and the length of the connecting rod are also included in optimal parameter set. The method was applied to the desired trajectory which followed a circle path and desired external wrench boxes as parallelepiped box for each pose in desired path. The

study has demonstrated success of the algorithm for designing a HCDPPR in finding optimal solution of given tasks. The PSO showed very good convergence for all the trial runs. The method developed should be very useful as a design tool as it guarantees the cable will always be in tension during the task. Potentially, the method developed may be applied to problems that required large workspace such as gait rehabilitation device in order to achieve optimal design. However, to implement this mechanism for large workspace, some practical aspects still need to be considered. The issues such as cable tangling and sacking need yet to be investigated. These topics will require more in-depth analysis and should be considered in future work.

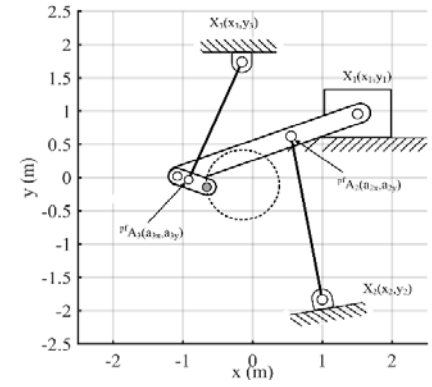

(a) 1st iteration

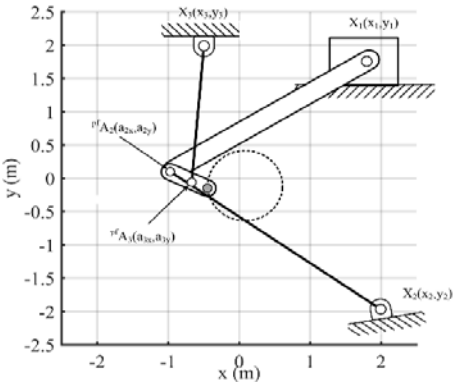

(b) 6th iteration

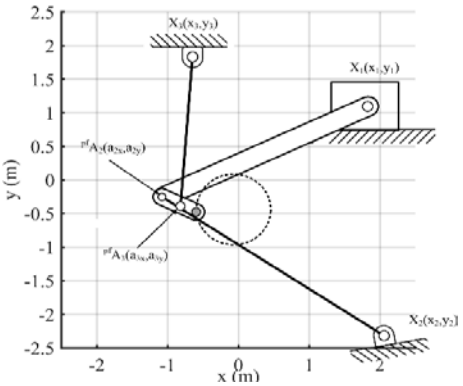

(c) 12th iteration

Fig.8. The configuration solution at ($\boldsymbol{P}^k$)

ACKNOWLEDGEMENT

This research was partially supported by The Royal Golden Jubilee Ph.D. Program (RGJPHD) Scholarship no. PHD/0101/2552 1.M.CM/52/G.1 and by Chiang Mai University's Mid-Career Grant 2014. The work was performed at the Motion and Control Laboratory, Chiang Mai University, Thailand.

REFERENCES

Azizian, K., and Cardou, P., "The Constant-Orientation Dimensional Synthesis of Planar Cable-Driven Parallel Mechanisms Through Convex Relaxations,"; Mechanisms and Machine Science: Cable-Driven Parallel Robots, Vol. 12 Springer, pp. 215-230 (2013).

Azizian, K., and Cardou, P., "The Dimensional Synthesis of Planar Parallel Cable-Driven Mechanisms Through Convex Relaxations,"; J. Mechanisms Robotics, Vol. 4, No. 3, pp. 031011 (2012).

Bosscher, P., Riechel, A. T., and Ebert-Uphoof, I., "Wrench-Feasible Workspace Generation for Cable-Driven Robots,"; IEEE Transaction on Robotics, Vol. 22, No. 5, pp. 890-902 (2006).

Bouchard, S., Gosselin, C., and Moore, B., "On the Ability of a Cable-Driven Robot to Generate a Prescribed Set of Wrenches,"; J. Mechanisms Robotics, Vol. 2, No. 1, pp. 011010 (2010).

Bruckmann, T., Mikelsons, L., Brandt, T., Hiller, M., and Schramm, D., "Design Approaches for Wire Robots,"; Proc. of ASME 2009 International Design Engineering Technical Conferences and Computers and Information in Engineering Conference, San Diego, California (2009).

Bryson, J. T., Jin, X., and Agrawal, S. K., "Optimal Design of Cable-Driven Manipulators using Particle Swarm Optimization,"; J. Mechanisms Robotics, Vol. 8, No. 4, pp. 041003 (2016).

Gouttefarde, M., "Characterizations of Fully Constrained Poses of Parallel Cable-Driven Robots: A Review,"; Proc. of ASME 2008 International Design Engineering Technical Conferences and Computers and Information in Engineering Conference, Brooklyn, New York (2008).

Hay, A., and Snyman, J.A., "Optimization of a Planar Tendon-Driven Parallel Manipulator for a Maximal Dexterous Workspace,"; Engineering Optimization, Vol. 37, No. 3, pp. 217-236 (2005).

Kulkarni, N. K., Patekar, S., Bhoskar, T, Kulkarni, O., Kakandikar, G. M., and Nandedkar, V.M., "Particle Swarm Optimization Applications to Mechanical Engineering-A Review,"; Materials today. Vol. 2. No. 4-5, pp. 2631-2639 (2015).

Marini, F., Walczak, B., "Particle Swarm Optimization (PSO). A Tutorial,"; Chemometrics and Intelligent Laboratory Systems,Vol.149B, pp.153-165 (2015).

Pham, C. B., Yeo, S. H., Yang, G., Kurbanhusen, M.S., and Chen, I.M., "Force-Closure Workspace Analysis of Cable-Driven Parallel Mechanisms,"; Mechanism and Machine Theory, Vol. 41, No. 1, pp. 53-69 (2006).

Roberts, R. G., Graham, T., and Trumpower, J. M., "On the Inverse Kinematics and Statics of Cable-Suspended Robots,"; Proc. of 1997 IEEE International Conference on Systems, Man, and Cybernetics, Orlando, Florida (1997).

Shen, H., Zhu, Y., Niu, B., and Wu, Q. H., "An Improved Group Search Optimizer for Mechanical Design Optimization Problems,"; Progress in Natural Science, Vol. 19. No. 1, pp. 91-97 (2009).

APPENDIX

$$\boldsymbol{M} = \begin{bmatrix} m_p + m_b + m_{pf} & -(m_{pf} + 0.5m_b)l_b \sin\beta & -m_{pf} b_p \sin\gamma \\ -(m_{pf} + 0.5m_b)l_b \sin\beta & (m_{pf} + 0.25m_b)l_b^2 + I_b & m_{pf} l_b p_b \cos(\beta - \gamma) \\ -m_{pf} b_p \sin\gamma & m_{pf} l_b p_b \cos(\beta - \gamma) & I_{pf} + m_{pf} b_p^2 \end{bmatrix}$$

$$\boldsymbol{N} = \begin{bmatrix} -(m_{pf} + 0.5m_b)l_b \cos\beta \dot{\beta}^2 + m_{pf} b_p \cos\gamma \dot{\gamma}^2 \\ m_{pf} b_p \sin(\beta - \gamma)\dot{\gamma}^2 \\ 0 \end{bmatrix}$$

$$\boldsymbol{G} = \begin{bmatrix} 0 \\ (m_{pf} + 0.5m_b) g l_b \cos\beta \\ m_{pf} g b_p \cos\gamma \end{bmatrix}$$

$$\boldsymbol{p} = [X_2 \quad Y_2 \quad X_3 \quad Y_3 \quad A_{2xf} \quad A_{3xf} \quad l_b \quad y_o \quad m_{pf} \quad b_f]^t$$

$$\boldsymbol{LB} = [\, X_{2m} \;\; Y_{2m} \;\; X_{3m} \;\; Y_{3m} \;\; A_{2xfm} \;\; A_{3xfm} \;\; l_{bm} \;\; y_{0m} \;\; m_{pfm} \;\; b_{fm} \,]^t$$

$$\boldsymbol{UB} = [\, X_{2M} \;\; Y_{2M} \;\; X_{3M} \;\; Y_{3M} \;\; A_{2xfM} \;\; A_{3xfM} \;\; l_{bM} \;\; y_{0M} \;\; m_{pfM} \;\; b_{fM} \,]^t$$